

DESIGNING OF A SINGLE AXIS SOLAR TRACKER USING A NON-PROGRAMMABLE INTEGRATED CIRCUIT

Jojit D. Aquino ¹

Received 08.05.2024.
Revised 15.01.2025.
Accepted 04.02.2025.

Keywords:

Accuracy, Efficiency, Op-Amp, Photo-voltaic module, Single Axis, Solar Tracker

ABSTRACT

The sun is the ultimate source of energy. However, harvesting its energy remains a challenge because of the limited efficiency of the available photovoltaic (PV) modules. This study employed the developmental and comparative-experimental research designs in developing a Single Axis Solar Tracker. Results of the study revealed that the newly developed solar tracker is a non-microcontroller based that utilizes an OP-Amp integrated circuit. The device helped the PV module harvest energy up to 9 sun-hour, an increase of 48.04% in harvested energy in a day. Moreover, the alignment of the solar tracker is almost the same with respect to the angle of elevation of the sun at noon time.



© 2025 Published by Faculty of Engineering

1. INTRODUCTION

The demand of using renewable energy is increasing day by day as these non-renewable sources (fossil fuels) impose negative effects to mankind and to the environment because of the large amount of carbon footprints they are emitting. In this regard, many researchers have introduced alternative sources of energy that provide a sustainable power/ electricity production that would not harm the environment. The alternative energy sources include solar, wind, hydro, geothermal and ocean tidal wave. They are called as renewable energy.

Consequently, many countries in the whole world have been using renewable energy as their source in power production. Among these nations, China, potentially the foremost contributor to global pollution, stands out as the

leading global investor in renewable energy, with significant investments both domestically and internationally (Climate Council, 2022; Energy Pedia, 2019).

In the Philippines, the renewable energy sector is continually expanding within our nation, presenting a tangible initiative to address the challenges posed by climate change, energy security, and energy accessibility (Domingo et al., 2021). Among the aforementioned renewable energy sources, solar energy stands out as the most environmentally friendly, contributing the least to climate pollution. Solar energy refers to electromagnetic energy, or solar radiation, transmitted by the sun, with approximately one billionth of it reaching the Earth. This solar radiation, fundamental to all terrestrial life, totals around 420 trillion kilowatt-hours, surpassing the collective energy consumption of humanity by several

¹ Corresponding author: Jojit D. Aquino
Email: jojit.aquino@unp.edu.ph

thousand times. It is approximated that each square kilometer (about 0.4 square miles) of land receives around 4000 kilowatts (4 megawatts) of solar energy daily, a quantity sufficient to meet the needs of a medium-sized town.

Furthermore, a prospective environmental benefit of solar power lies in its capacity to mitigate CO₂ emissions, primarily as a clean and sustainable energy source (Queypo & Gonzales, 2021). Solar power diverges from dependence on the combustion of fossil fuels or other substances, harnessing electrons from the sun's energy to generate power. Consequently, the utilization of solar energy in homes avoids the production of greenhouse gases during energy generation.

Likewise, many studies revealed that using solar power has now proved to be highly beneficial for financial matters. This system may reduce electricity bills since the solar power system generates some of the electricity needed at home. Moreover, there is a possibility to receive payments from the Electricity Company for the surplus generated energy to be exported back to the grid.

Meanwhile, a solar power system comprises the four main parts to operate. 1) The solar panel (photovoltaic), which converts the sun's light energy into useable electric energy; 2) the charge controller, which regulates the voltage and current being fed to the battery bank to prevent overcharging; 3) the Battery, which serves as the storage of power harnessed from the sun through the solar panel; and, 4) the Direct Current (DC) to Alternating Current (AC) power inverter (preferably the pure sinewave inverter) which converts the low voltage DC from the battery into an AC with higher voltage (220V), (Solar Online Australia, 2019).

Despite the vastness of the sun's energy, harvesting it presents a challenge due to the limited efficiency of solar cells, as noted by Otieno (2019), with most commercially available solar panels achieving efficiencies between 10 to 20 percent. This inefficiency necessitates many panels to meet energy demands or investing in a single system with high output, albeit at a substantial cost.

When setting up fixed-mount solar panels, it is crucial to determine their correct orientation and tilt to ensure optimal exposure to sunlight. Given that the country is situated north of the equator, the sun predominantly travels from the south throughout most of the year. In the case of Metro Manila, positioned within the 14° to 15°N latitude range, the sun moves north from May to August and south from September to April. Consequently, the sun is predominantly in the south for the majority of the year, making it advisable for solar panels to face in that direction.

Furthermore, Malicdem (2015) as cited by Beale (2022), introduced a formula to calculate the ideal tilt for fixed solar panels: $\text{latitude} \times 0.812 = \text{angular inclination facing}$

south. For instance, considering the Bolinao Lighthouse located at 16.30704°N latitude, applying the formula suggests that its solar panels should face south at an angle of 13.24131648° from the horizontal.

However, for optimal effectiveness, solar panels should be oriented perpendicularly to the sun's rays (Honsberg & Bowden, 2019). The output of a fixed-mount solar panel undergoes significant fluctuations throughout the year and even daily due to the Earth's rotation, which causes the sun to move across the sky, resulting in sunrise and sunset. The sun's position varies in the hemisphere as it travels at different inclinations from north to south, depending on the time of the year. This variation is attributed to the Earth's axial tilt of 23.4°. Consequently, the sun traverses the sky from east to west with a north-south deviation of 46.8 degrees throughout the year, reaching its maximum angle with direct rays on December 21st at 23.4° degrees south latitude (Tropic of Capricorn) and 23.4° north latitude (Tropic of Cancer) on June 21st. Moreover, the sun reaches its northernmost point during the summer solstice on June 21 at 23.4 degrees north, and its southernmost point during the winter solstice on December 21 at 23.4 degrees south (Beale, 2022).

Thus, to ensure maximum exposure to sunlight, a solar panel needs to adjust its position. To tackle this challenge, a solar tracker comes into play. This device enhances the exposure of solar panels to sunlight throughout the day by accurately aligning the panel with the sun's array, leading to a potential increase in power output by up to 40 percent.

As outlined by Mondal (2022), solar tracker systems fall into two categories. Firstly, the single-axis horizontal tracker, which typically shifts from east to west, mirroring the sun's journey across the sky from morning to evening. This option is well-suited for locations near the equator, where the sun's apparent position experiences minimal variation. Secondly, the dual-axis tracker incorporates both vertical and horizontal pivots. It proves to be the superior choice in regions where the sun's position undergoes seasonal changes throughout the year. Although more efficient than the single-axis alternative, the dual-axis tracker comes with a higher cost.

For a solar tracker to operate efficiently, it relies on three primary components: light sensors, actuators/servo motors, and controllers. The prevalent light sensor employed in solar trackers is the light-dependent resistor (LDR). An LDR is a passive component with resistance that varies inversely with the intensity of light falling upon it. Typically, the LDR exhibits very high resistance, reaching values as high as mega ohms (Ω) in darkness. However, its resistance undergoes a significant drop to a few hundred ohms when exposed to light. In low-light conditions, the LDR's resistance is high, and conversely, it decreases when light levels are elevated.

Furthermore, light-dependent resistors (LDRs) are crafted from semiconductor materials to impart light-sensitive characteristics. While various materials are suitable, a commonly employed substance for these photoresistors is cadmium sulfide (CdS). However, the utilization of cells made with cadmium is now limited in Europe due to environmental concerns associated with cadmium usage. Similarly, restrictions also apply to cadmium selenide (CdSe). Alternatives include materials such as lead sulfide (PbS) and indium antimonide (InSb) (Otieno, 2019).

A linear actuator is responsible for moving the panel either upside down or in a clockwise/counterclockwise direction, generating motion in a straight line. Various types of linear actuators exist, including mechanical, hydraulic, pneumatic, and more, with the mechanical variant being the most common. Mechanical linear actuators typically utilize a screw and an electric motor, rotating the screw to produce linear motion. Those employing acme screws are self-locking, a feature absent in ball screws. Some linear actuators incorporate a variable resistor that changes value based on the stroke's location, providing feedback data on the stroke's position. Due to their ease of control and relatively low cost, linear actuators find widespread use in home solar tracking applications. Achieving horizontal rotation involves mounting the base of the linear actuator on a tracker frame and connecting the stroke to the solar panels.

Moreover, the primary function of the controller is to receive data from sensors, process it, and send signals to operate the motors and actuators. Simplistically, a human could substitute for a controller by manually observing the sun's position and adjusting the tracker for optimal energy capture. However, this approach is impractical for prolonged periods or in scenarios involving multiple trackers, such as in a solar power plant. Consequently, automated controllers have become essential. These controllers must also consider actions to take when the sun sets, when wind conditions are excessive, or during other physical circumstances (Otieno, 2019).

Nevertheless, solar trackers are not new to the ears of some individuals. These have been there since the 1980s. Many researchers have constructed their version. And all were made successful objectively. Accordingly, most of their versions were microcontrollers and electro-optical sensor-based. In the study of Anusha et al. (2013), the results of his single axis solar tracking system based on a real-time clock using an ARM processor showed that there was an increase of 40% of the energy received by the solar panel from the sun. In contrast, the constructed version for the solar tracker in this paper was a non-microcontroller version that utilized, instead, a very common quadruple operational amplifier (Op Amp) integrated circuit (IC), which serves as the brain of the entire tracking system. This op amp does not require pre-programmed data to install it.

In this regard, the researcher intended to design and construct a non-microcontroller single-axis solar tracker using a very common quadruple operational amplifier (Op Amp) integrated circuit (IC) which serves as the brain of the entire tracking system. This op amp does not require pre-programmed data to install in it. This version helps lessen the production cost. Microcontroller chips are more expensive compared to the operational amplifier IC. Moreover, since the system has no microcontroller chip that require pre-programming, so when it subjects for repair, there is no need to have special tool and equipment for programming like computers, thus this version also helps lessen the maintenance cost.

The study also covered the testing of the performance of the system in terms of its Efficiency (by comparing the amount of energy harvested by the solar panel with the tracking system, and with the fixed solar panel) and Accuracy (that is how accurate is the calibration made to the tracker to position the PV module to be at 90 degrees during noon-sun angle with respect to the location of the t tracker).

2. METHODOLOGY

This study employed the developmental research design, whereby the researcher developed a single-axis solar tracker that utilized an operational amplifier integrated circuit as the system's central controller (Buen et al., 2022). In essence, Development Research is characterized as the systematic examination of creating, designing, and assessing instructional programs, processes, and products that must adhere to standards of reliability and efficiency. Frequently, development research revolves around scenarios where the analysis and description of the product development process take place, culminating in the evaluation of the final product (Richey, 2019).

Also, the comparative-experimental research design was used in this study, whereby the researcher compared the two data sets collected during the experiment (Lau, 2019). These two sets of data were the recorded power generation of the PV modules with and without a tracker and then compared to see the effects of the constructed solar tracker on the PV modules.

2.1 Procedures

Figure 1 shows the flowchart that illustrates the steps in the design and development of an Op Amp Based Single Axis Solar Tracker.

The first step was the design conceptualization, whereby the researcher planned the design of the system, particularly the circuit used and the frame comprising the mechanism of a single-axis solar tracker. In designing the schematic diagram PCB layouts of the device, the researcher used the software application Proteus 8

Professional, a circuit simulator. The value per component was determined via computations. After it was designed, a simulation was made through the apps to see whether it worked. Moreover, before it was transferred to the printed circuit board, actual simulation was also made using the breadboard. Some modifications to the circuit design and adjustments to the value of specific components were made when flaws were observed during the simulation process until the circuit was made perfectly. Below is designed schematic diagram of the solar tracker module.

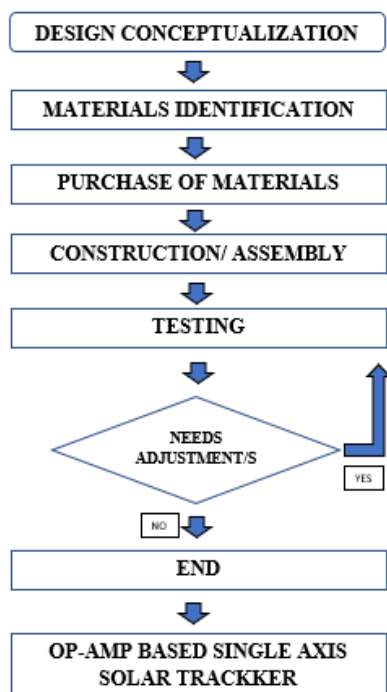


Figure 1. Flowchart in Developing an Op Amp Based Single Axis Solar Tracker

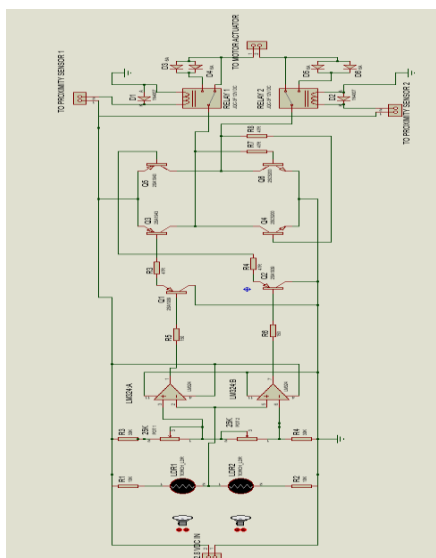


Figure 2. Schematic Diagram of an Op-Based Single-Axis Solar Tracker

In the Second step, the researcher made a master list of the materials used for the project. In identifying these materials needed, the researcher must look into the correct specifications of each to ensure that the device/system to be constructed will deliver its maximum capacity without breaking down the components easily.

The third step was to purchase the final list of supplies and materials needed. During the procurement, the researcher first checked the availability of these materials from the list in the local market, and if some materials were unavailable locally, purchasing from overseas via online shopping was needed. However, in doing so, the researcher looked at the possible lowest price with high-quality materials. Most of the materials for the tracker frame were bought from Junkshop to minimize the cost.

The fourth step was the construction and assembly of the system. Based on the planned designs and schemes, the researcher constructed/assembled first the frame for the tracker, then the tracker module. After constructing/assembling the module circuits, initial testing was followed to determine if it worked properly before placing it permanently in its case.

Figures 3 and 4 show the isometric and the exploded view of the constructed Solar Tracker Frame design, respectively. These served as the guide for the researcher in fabricating the frame.



Figure 3. Isometric Drawing of the Solar Tracker Mechanism



Figure 4. Exploded View of the Solar Tracker Mechanism

The following figures (figure 4 to 8) show the processes in constructing the solar tracker frame.



Figure 4. Cutting process



Figure 5. Welding process



Figure 6. Drilling process



Figure 7. Grinding process



Figure 8. Painting process

In constructing/assembling the solar tracker module (figure 9 to 14), the following figures show the processes in lay outing of the Printed Circuit Board (PCB) and Mounting of the Components to the PCB)

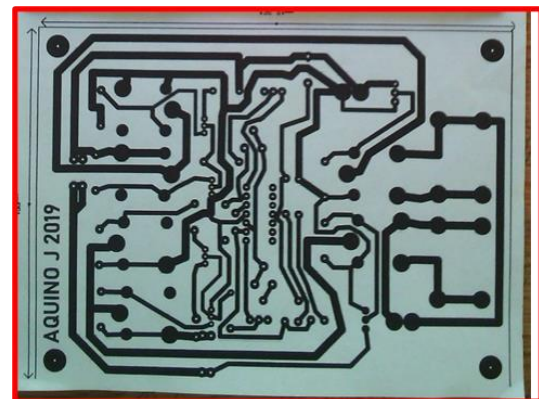


Figure 9. PCB layout of the Solar Tracker Module



Figure 10. Removing the unused area of the layout

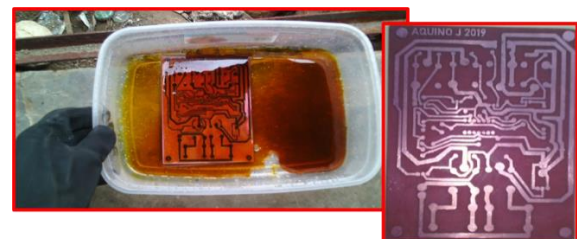


Figure 11. PCB Etching Process



Figure 12. PCB Boring Process



Figure 13. Mounting of Electronic Components

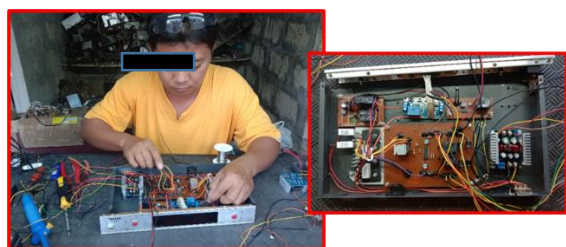


Figure 14. Assembling of the Solar Tracker Module

For the fifth step, the device was subjected to sets of dry runs to assess its technical performance regarding efficiency and reliability. There were again adjustments/calibration performed. When the system passed for testing by the researcher, commission-testing was followed for two weeks. The system was installed/set up at the researcher's house to run certain loads the whole day. There was an every-hour monitoring (from 7 AM to 5 PM for one week) regarding the amount of energy harvested by the solar panel with the tracking system, and another one week observation for the harvested energy by the solar panel without a tracking system. The results were compared to determine the efficiency of the constructed solar tracker.

The following figures (figure 15 to 17) show the captured photos of the solar meter indicating the Power generated by the PV modules during the testing process



Figure 15. Power Generation of the PV Module at 8AM (With Tracker vs Without Tracker)



Figure 16. Power Generation of the PV Module at 1PM (With Tracker vs Without Tracker)



Figure 17. Power Generation of the PV Module at 5PM (With Tracker vs Without Tracker)

2.2 Analysis of Data

In terms of its technical performance, the system was tested its efficiency and accuracy during sunny days in order to determine its maximum capacity. Its efficiency was analyzed by simply comparing the generated power or harvested energy of the solar panel having a tracker and without a tracker at the same time. Also, its accuracy in terms of tracking the position of the sun by measuring the tilt-angle of the solar panel with respect to the arrays of the light of the sun.

3. RESULTS AND DISCUSSION

3.1 Designing and constructing of an Op -Amp Based Single-Axis Solar Tracker

3.1.1 The Schematic Diagram of the Solar Tracker and its principle of operation

Under the designing process, the researcher designed first the schematic diagram with computation using the software application Proteus 8 Professional.

In Figure 2 shows the schematic diagram of the solar tracker. It comprises a comparator IC LM324 and utilized the two comparator configurations. For loop LM324:A is configured as “inverting comparator” since the reference voltage is applied to its non-inverter terminal (pin 3), and the input voltage is applied to its inverting terminal (pin 2), and the output is taken from pin 1. For loop LM324:B is configured as “non-inverting comparator” since the reference voltage is applied to its inverting terminal (pin 6), and the input voltage is applied to its non-inverting terminal (pin 5), and the output is taken from pin 7. The reference voltage at pin 3 is set to 7.2V, and 4.8V at pin 6. These reference voltages can be achieved by simply adjusting the two variable resistors labeled POT₁ and POT₂. Loop through R₃-POT₁-POT₂-R₃ is a voltage divider circuit which is responsible for providing the two reference voltages. Now, the two input voltages at pins 2 and 5 is connected to the center point of the two LDR’s with R₁ and R₂ which is also another voltage divider circuit. Since the voltage supply (V_{CC}) is 12.8V, when the two LDRs receive the same amount of light through them, the voltage at its center will be equal to 6.4V. With that initial voltage measurements, comparator LM324:A has a high or almost 12.8V output at pin 1 since terminal

(+) is greater than terminal (-). While comparator LM324:B has also high output at pin 7 since its (+) terminal is greater than its (-) terminal. At this state, the motor is in off position.

When LDR₁ receives more light than LDR₂, it offers lower resistance than LDR₂, providing a higher input voltage (say 10V) to both comparators at pins 2 and 5, respectively. As a result, output pin 1 of comparator LM324:A goes low (while comparator LM324:B remains high) to rotate motor M₁ in one direction (say, anti-clockwise) and turn the solar panel.

When LDR₂ receives more light than LDR₁, it offers lower resistance than LDR₁, giving a lower input voltage (say 2V) to both comparators at pins 2 and 5, respectively. As a result, output pin 7 of comparator LM324:B goes low (while the other comparator remains high) causing motor actuator to rotate in the opposite direction (say, clock-wise) and the solar panel turns.

When one of the two comparators' output goes low, say pin 1, Q₁ will be energized through its base bias resistor R₅. Also, output transistors Q₃ and Q₆ will be triggered through their base bias resistors R₃ and R₇, respectively. During this state, the output voltage at point A will be positive while point B will be negative, which in turn the motor actuator rotates in one direction, (say counter-clockwise). On the other hand, if pin 7 goes low (while pin 3 goes high), Q₂ will turn on via base bias resistor R₆ causing the other output transistors Q₅ and Q₄ be energized through their base bias resistors R₄ and R₈. At this state, point A becomes negative, while point B becomes positive resulting to rotate the motor actuator in opposite direction, say clockwise.

The limit switch stage of the circuit uses blocking diodes and inductive proximity sensors to activate the relays in order to cut off the supply of the motor actuator. During the operation, say at point A is positive and point B is negative, the current will flow through the "normally closed" terminals of the two relays going to the motor actuator as it rotates counter clockwise. While the motor is turning, the whole solar panel also moves towards (say to the west). Once the solar panel reaches its maximum tilt angle, one of the proximity sensors (PS) (say PS₁) which are installed in the actuator, will be energized and relay1 will be activated, which in turn the line of point A will be transferred to the "normally open" terminal of relay1. As a result, the motor will stop since current will not flow anymore going to the motor because of the blocking diodes D₃ and D₄. Then, in the afternoon, when the sun totally sets, point A becomes negative while point B becomes positive (since the two comparators' output have changed too). Then the motor actuator rotates to opposite direction causing to deactivate the Relay₁, and moves the solar panel towards east to be ready again for the next day. And, the moment the solar panel reaches its maximum tilt angle to the east, again the proximity

sensor 2 (PS₂) will be energized to activate Relay₂. When Relay₂ is activated, line of point B will be shifted to its "normally open" terminal which causes the motor to stop since the current will not flow anymore through it because of the two blocking diodes D₅ and D₆. And, D₁ and D₂ are used to protect the proximity sensor switch from the back emf induced by the coil of the relay when it turns off. It clips the high voltage induced by the relay coil.

3.1.2 The Constructed Solar Tracker Frame/ Mechanism

Figure 18 shows the actual picture of the constructed single axis solar tracker system



Figure 18. Actual Picture of the Single Axis Solar Tracker System

In figure 4, shows the exploded view of the constructed frame of the single axis solar tracker system. The frame was made up of steel/metal bought from junkshop. It is 180cm tall, and the railings measure 200cm x 164cm. Its post (4) was made out of two channel bars (2"x3"x 1/4") with a length of 173cm, welded together to form a square. The 46cm x 29cm base (2) is a 1" thick metal sheet. The "T" formed square bar (12) which is made out of two angle bars (2"x2"x 1/4") that are welded together, is attached to the pinnacle of the post with bushing (24) in order to move the panel from south to north via the adjustable metal tubing support. This adjustable (south to north) support (6) is made out of two metal tubes with different in diameter (3/4" and 1/2") so that the smaller one can be fit inside the other. They are connected with a threaded rod and nut, so when one of the metal tubes turns either clock wise or counter clock wise, the support will extend or compress its length causing the tilt of the solar panel adjust from south to north. The maximum tilt to the south is approximately 45-50 degrees from flat

position. And about 10 degrees to the north. Also, this “T” formed square bar (12) is responsible for holding the metal railings (14) of the panel. While the aluminum railings (18) are attached to the metal railings (14). And to make the panel movable facing from east to west, 3 pcs of pillow blocks (20) were used. Then the 3 metal railings(14) of the panel is attached to a channel bar (16) where the pillow blocks(20) are fixed using bolts and nuts. For the “east to west” support of the panel, a linear actuator is used which is responsible for tilting the solar panel from east to west automatically with a maximum tilt angle of 30 degrees from flat position. This actuator is made out of scissor jack (10) and a wiper motor (8) to rotate the rod of the scissor jack causing it to extend or compress which in turn the panel moves from east to west. The maximum tilt of the panel either to the east or to the west is around 30 degrees from flat position. To monitor the tilt angle, a “protractor” (22) is attached to the channel bar (16) of the metal railings (14). The LDR sensor frame (24) is attached to the center aluminum rail. And the solar panel (26) is then placed on top of the aluminum railings (18).

3.1.3 The Constructed Solar Tracker Module

Figures 19 and 20 show the actual picture of the finished tracker module. The casing is made up of metal, and aluminum. This box was from a salvaged microphone transmitter module. All sidings and openings were sealed using silicon to prevent from moist and water penetration of the module. In front of it can be accessed the main power switch, and the two button switches used to adjust or position the panel manually when subject for maintenance, example- cleaning the panel. At the back of the module can be found the terminal connectors wherein the proximity sensors, LDR sensors motor actuator, and input supply are connected. This module is mounted at the post of the solar tracker frame.



Figure 19. Actual Picture of the Solar Tracker Module (Front View)



Figure 20. Actual Picture of the Solar Tracker Module (Back View)

3.2 Testing the performance of the Solar Tracker in terms of its Efficiency and Accuracy

3.2.1 Testing the efficiency by comparing the Power Generation of the PV Module (With Tracker VS. Without a Tracker)

Table 1 and figure 21 show the result of comparison regarding the harvested energy of the solar panels or PV module with tracker and without a tracker. The values of power indicated in table 1 was the average power generated by the 2 units of PV module (300 watts each module) which was conducted in a week observation from 7:00 AM to 5:30 PM (with a tracker; and without a tracker at the same time and they were both positioned 15-20 degrees tilt facing south). As depicted in the table, when the PV module is equipped with a tracker, it could already harvest as high as 197.3w in as early as 8 o’clock in the morning, and can still produce 169.5w at 5 o’clock in the afternoon, whereas, if without tracker, is only 41.4w and 22w respectively.

Table 1. Power Generation of the PV Module (With Tracker VS. Without a Tracker)

Time	With Tracker	Without Tracker
7AM-8AM	57.4w- 197.3w	12.1w-41.4w
8AM-9AM	197.3-338.7w	41.4w-122.3w
9AM-10AM	338.7w-418.7w	122.3w-241w
10AM-11AM	418.7w-432.2w	241w-373.9w
11AM-12NN	432.2-430.3w	383.1w-424.2w
12NN-1PM	430.3w-434.6w	424.2w-434.1w
1PM-2PM	434.6w-423.6w	434.1w-409.9w
2PM-3PM	423.6-405.1w	409.9w-307.3w
3PM-4PM	405.1w-350.5w	307.3w-246.8w
4PM-5PM	350.5w-169.5w	246.8w-22w
5PM-5:30PM	169.5w-60w	22w-10w

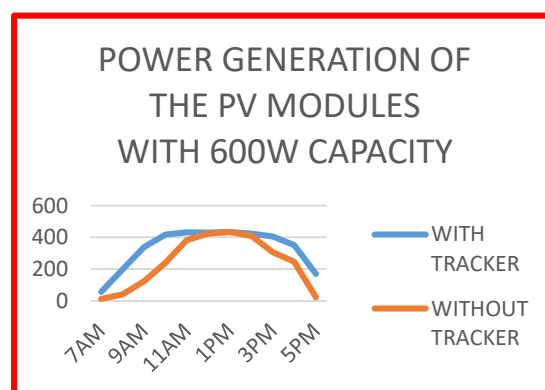


Figure 21. Power Generation of the PV Module (With Tracker VS. Without a Tracker)

This means that the tracker helps maximizing the “sun-hour” into 9 hours (8am – 5pm) for the PV to harvest energy. Moreover, it can be noticed that the system (both with tracker and without a tracker) have almost the same harvested power at 12NN to 1PM because the sun is perpendicularly above the PV module, so both will receive almost the same amount of light from the sun.

Also, the highest power generation being recorded is around 434w at 1 o'clock PM. This means that this is the "noon sun angle" where the sun appeared 90 degrees in the sky with respect to the location of the System.

Table 2 compares the amount of energy harvested by the PV modules, with a tracker and without a tracker. The data recorded was split into two period- 7AM to 12NN; and 12NN to 5:30PM. It can be observed from the table that the PV modules generate more energy in the afternoon (from 12NN to 5:30PM) because they have more number of hours exposed to the sun. Based from the total energy generated/harvested, there is a difference of 1.121KWh. This means that the tracker efficiently maximized the number of sun-hour for the PV modules to harvest energy from the sun by **48.04% efficiency**, $(1.121KWh / 2.333KWh) \times 100\%$.

Table 2. Energy Generated/Harvested by the System in a Day

TIME PERIOD	WITH TRACKER	WITHOUT A TRACKER
7AM – 12NN	1.605KWh	1.031KWh
12NN- 5:30PM	1.849KWh	1.302KWh
TOTAL	3.454KWh	2.333KWh

Many studies proved that a solar tracker could maximize the sun-hour period of the PV module to generate energy. In the study of Racharla, and Rajan (2019) entitled "solar tracking system- A review", he presented many research studies conducted by different authors regarding the efficiency of the solar tracker. Anusha et al. (2013), as cited by Racharla, and Rajan (2019), compared the fixed PV panel and single axis solar tracking based on real time clock(RTC) using ARM processor. The experiment is conducted using both fixed and tracking system for 6 days. The results show that the solar tracking system increased the efficiency around 40% and energy received from the sun is improved from 9.00AM to 6.00 PM. Another study also compared the efficiencies of static panels and tracking systems of single axis and dual axis fixed mount. The readings were taken from morning 8 AM to evening 6 PM for fixed panel, single axis tracker and dual axis tracker for every one hour. The results say the efficiency of the single axis tracking system over that of the static panel is calculated to be 32.17% and dual axis tracking system over that of the static panel is calculated to be 81.68%. The same study compared the solar tracking PV panel with a fixed PV panel in terms of electric energy output and efficiency. The proposed device automatically searches the optimum PV panel position with respect to the sun by means of a DC motor controlled by an intelligent drive unit that receives input signals from dedicated light intensity sensors. The solar tracking PV panel produced more energy than fixed one with about 57.55%.

3.2.2 Testing the Accuracy of the Solar Tracker

In this study, accuracy means that is how precise is the calibration made to the tracker to position the PV module

to be at 90 degrees during noon-sun angle with respect to the location of the tracker.

To calibrate the solar tracker, the researcher aimed to position the PV module in 90 degrees (see figure 22) during noon sun angle. A noon sun angle is the angle of the sun when it appears in the sky at 90 degrees position with respect to the location of the observer (latitude). And it is calculated using the formula "Noon Sun Angle" = 90 degrees minus Zenith angle; and the formula for "Zenith angle" = subsolar point \pm latitude..



Figure 22. PV module positioned in 90 degrees

During the experiment dated February 07, 2023, the subsolar point for this day was found in 16.4 degrees South; 108.1 degrees East at about 1:00 o'clock PM. The tracker was mounted in Parada Santo Domingo Ilocos Sur. The latitude and longitude coordinates of this address is 17.66 degrees North; 120.42 degrees East, respectively.

Thus, the computation for the noon-sun angle is presented below.

Given Data:

$$\begin{aligned} \text{Subsolar point (feb.7, 2023)} &= \mathbf{16.4 \text{ degrees S}} \\ \text{Latitude} &= \mathbf{17.66 \text{ degrees N}} \end{aligned}$$

Find Zenith Angle: (note, if the subsolar point and the latitude belongs to the same hemisphere, subtract; if they are in different hemisphere, add.)

$$\begin{aligned} \text{Zenith Angle} &= \text{subsolar point} + \text{latitude} \\ &= 16.33 + 17.66 \\ &= \mathbf{34.06 \text{ degrees}} \end{aligned}$$

Then, find Noon Sun Angle:

$$= 90 - 34.06$$

$$= \mathbf{55.94 \text{ degrees}}$$

(this is the angle of elevation of the sun wherein it appears 90 degrees on the sky, with respect to the latitude at 1:00PM).

Then, in the same day, the researcher conducted actual experiment regarding the angle of elevation of the sun by making such actual computations using the shadow technique that could be able to determine the angle of elevation using one of the trigonometric functions.

The researcher used a stick measured 26.5cm, and positioned vertically and placed it under the sun (see figure 23), and checked the shadow of the stick until it

reached 18cm long at around 1:00 o'clock in the afternoon. This length of shadow gives an angle of elevation of 55.81 degrees which is very near to the computed noon sun-angle, (55.94 degrees). In figure 24 shows the computation of the angle of elevation of the sun. And finally, the researcher checked the position of the tracker and it was at 90 degrees position at 1:00 PM, see Figure 25.



Figure 23. Shadow technique for measuring angle of elevation of the sun Dated February 07, 2023 @ 1:00PM

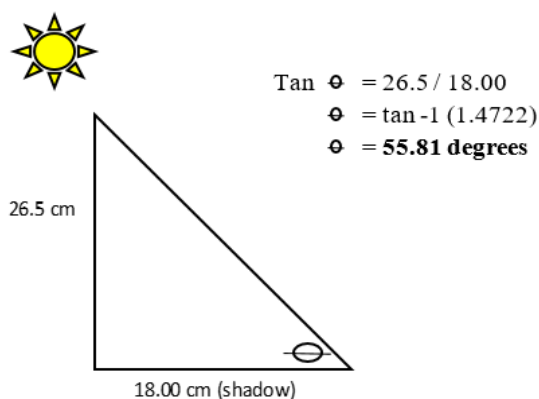


Figure 24. Computation of the angle of elevation of the Sun



Figure 25. Alignment of the PV module during Noon-Sun Angle @ 1PM on February 07, 2023

With these results, the alignment is said to be very near to 100% accurate that the solar panel is perpendicular to the sun's rays at noon sun angle. And, the accuracy of the tracker to position itself with respect to the sun is almost perfect.

4. CONCLUSION

The developed non-microcontroller based solar tracker that utilized an Op-Amp integrated circuit has a comparable performance to that of the existing programmable type, but the first is more economically efficient (Aquino, 2018). Moreover, the developed solar tracker effectively maximized the number of "sun-hour" for the PV module resulting to have an additional of 48.04% of the total harvested energy from the sun.

5. RECOMMENDATIONS

Adopting the developed solar tracker is recommended to optimize the capability of the PV module or solar panel in collecting energy from the sun. Moreover, further study to construct a dual axes solar tracker may be conducted to determine also its efficiency over the constructed one.

References:

- Aquin, J. D. (2018). Effectiveness of a locally assembled mobile phone-based anti-theft device. *International Journal of Scientific & Engineering Research*, 9(9), 1460. <https://www.ijser.org/researchpaper/EFFECTIVENESS-OF-A-LOCALLY-ASSEMBLED-MOBILE-PHONE-BASED-ANTI-THEFT-DEVICE.pdf>
- Beale, A. (2022, January 12). Solar panel tilt calculator. Footprint Hero. <https://footprinthero.com/solar-panel-tilt-angle-calculator>
- Buen, D. V., Tactay, N. T., & Alasaas, J. D. (2022). Predictors of programming abilities of information technology students in UNP. *The Vector: International Journal of Emerging Science, Technology and Management*, 31(1). <https://vector.unp.edu.ph/index.php/1/article/view/293>
- Climate Council. (2022, August 15). 11 countries leading the charge on renewable energy. <https://www.climatecouncil.org.au/11-countries-leading-the-charge-on-renewable-energy/>
- Domingo, J. C., Raboy, M. R., & Ramos, J. C. (2021). Oyster farming in Ilocos Sur, Philippines. *The Vector: International Journal of Emerging Science, Technology and Management*, 30(1). <https://vector.unp.edu.ph/index.php/1/article/view/69>
- Energy Pedia. (2019). Philippines energy situation. https://energypedia.info/wiki/Philippines_Energy_Situation
- Honsberg, C. B., & Bowden, S. G. (2019). Properties of sunlight/elevation angle. PV Education. <https://www.pveducation.org/pvcdrom/properties-of-sunlight/elevation-angle>

- Lau, F. C. M. (2017). Methods for comparative studies. In F. Lau & C. Kuziemy (Eds.), *Handbook of eHealth evaluation: An evidence-based approach*. University of Victoria. <https://www.ncbi.nlm.nih.gov/books/NBK481584/>
- Mondal, P. (2022, June 8). Solar tracker. Medium. <https://medium.com/@pratyushmondalpm007/solar-tracker-1a0d32d23e3d>
- Otieno, O. R. (2015). *Solar tracker for solar panel* [Unpublished bachelor's thesis]. University of Nairobi. <https://www.scribd.com/document/326576664/Solar-Tracker-for-Solar-Panel>
- Queypo, R., & Gonzales, L. R. (2021). Integrating climate smart development through bioclimatic planning and principles: The case of the World Heritage City of Vigan, Philippines. *The Vector: International Journal of Emerging Science, Technology and Management*, 30(1). <https://vector.unp.edu.ph/index.php/1/article/view/77>
- Racharla, S., & Rajan, K. (2017). Solar tracking system – a review. *International Journal of Sustainable Engineering*, 10(2), 72–81. <https://doi.org/10.1080/19397038.2016.1267816>
- Richey, R. C. (1994). Developmental research: The definition and scope. *Educational Resources Information Center (ERIC)*. <https://eric.ed.gov/?id=ED373753>
- Solar Online Australia. (2019). Solar system basics – How solar power works! Basic system components. https://www.solaronline.com.au/solar_system_basics.html

Jojit D. Aquino

University of Northern Philippines
College of Teacher Education
Philippines
jojitt.aquino@unp.edu.ph
ORCID 0009-0004-7321-6977
